Available online at www.sciencedirect.com
SCIENCE DIRECT®
Geochimica et Cosmochimica Acta 70 (2006) 3943–3956
Geochimica
www.elsevier.com/locate/gca

Enhanced late gas generation potential of petroleum source rocks via recombination reactions: Evidence from the Norwegian North Sea

Michael Erdmann [a,*], Brian Horsfield [b]

[a] Norsk Hydro Research Center Bergen, Sandsliveien 90, N-5020 Bergen, Norway
[b] GeoForschungsZentrum Potsdam, Telegrafenberg B425, D-14473 Potsdam, Germany

Received 11 February 2005; accepted in revised form 7 April 2006

Abstract

Gas generation in the deep reaches of sedimentary basins is usually considered to take place via the primary cracking of short alkyl groups from overmature kerogen or the secondary cracking of petroleum. Here, we show that recombination reactions ultimately play the dominant role in controlling the timing of late gas generation in source rocks which contain mixtures of terrigeneous and marine organic matter. These reactions, taking place at low levels of maturation, result in the formation of a thermally stable bitumen, which is the major source of methane at very high maturities. The inferences come from pyrolysis experiments performed on samples of the Draupne Formation (liptinitic Type II kerogen) and Heather Formation (mixed marine–terrigeneous Type III kerogen), both Upper Jurassic source rocks stemming from the Norwegian northern North Sea Viking Graben system. Non-isothermal closed system micro scale sealed vessel (MSSV) pyrolysis, non-isothermal open system pyrolysis and Rock Eval type pyrolysis were performed on the solvent extracted, concentrated kerogens of the two immature samples. The decrease of C_{6+} products in the closed system MSSV pyrolysis provided the basis for the calculation of secondary gas (C_{1-5}) formation. Subtraction of the calculated secondary gas from the total observed gas yields a "remaining" gas. In the case of the Draupne Formation this is equivalent to primary gas cracked directly from the kerogen, as detected by a comparison with multistep open pyrolysis data. For the Heather Formation the calculated remaining gas formation profile is initially attributable to primary gas but there is a second major gas pulse at very high temperature (>550 °C at 5.0 K min^{-1}) that is not primary. This has been explained by a recondensation process where first formed high molecular weight compounds in the closed system yield a macromolecular material that undergoes secondary cracking at elevated temperatures. The experiments provided the input for determination of kinetic parameters of the different gas generation types, which were used for extrapolations to a linear geological heating rate of 10^{-11} K min^{-1}. Peak generation temperatures for the primary gas generation were found to be higher for Heather Formation (T_{max} = 190 °C, equivalent to R_o appr. 1.7%) compared to Draupne Formation (T_{max} = 175 °C, equivalent to appr. R_o 1.3%). Secondary gas peak generation temperatures were calculated to be 220 °C for the Heather Formation and 205 to 215 °C for the Draupne Formation, respectively, with equivalent vitrinite reflectance values (R_o) between 2.4% and 2.0%. The high temperature secondary gas formation from cracking of the recombination residue as detected for the Heather Formation is quantitatively important and is suggested to occur at very high temperatures (T_{max} approx. 250 °C) for geological heating rates. The prediction of a significant charge of dry gas from the Heather Formation at very high maturity levels has important implications for petroleum exploration in the region, especially to the north of the Viking Graben where Upper Jurassic sediments are sufficiently deep buried to have experienced such a process.

1. Introduction

Natural gases fall into two basic categories, biogenic and thermogenic. Quantitatively more significant are the thermogenic gases which form via a combination of chemical reactions and physical fractionation processes in sedimentary basins (Wiese and Kvenvolden, 1993). Thermogenic gas is generated and expelled during the thermal maturation of organic matter residing in shales and coals. The gas generated directly from macromolecular precursors (kerogen, polar bitumen) is defined as primary,

* Corresponding author. Fax: +47 5599 5704.
E-mail address: Michael.Erdmann@hydro.com (M. Erdmann).

0016-7037/$ - see front matter © 2006 Elsevier Inc. All rights reserved.
doi:10.1016/j.gca.2006.04.003

whereas that generated from oil (mainly hydrocarbons) is termed secondary. Gas–oil ratio (GOR) is initially low in the generation products from typical marine source rocks and higher for coals and terrestrially influenced shales, but at more extreme levels of maturity GOR values are high for all source rocks (England and Mackenzie, 1989; Cornford, 1994; Santamaria-Orozco and Horsfield, 2004). This is because the primary methane-forming moieties in heterogeneous kerogens, being thermally stable, are the last to crack (Mackenzie and Quigley, 1988; Horsfield, 1989; Krooss et al., 1993), and because secondary gas is generated from unexpelled oil (Tissot and Welte, 1978; Monin et al., 1990; Dieckmann et al., 1998). Gas yields from in-source secondary cracking of unexpelled oil are highest where oil expulsion efficiencies are low, this being associated with leaner source rocks (<10 mg HC/g rock; Cooles et al., 1986. Also see Jones, 1980; Pepper and Corvi, 1995; Mann et al., 1997). Gas may also be generated from the thermal degradation of reservoired crude oil, but, whatever the crude oil type or the geological heating rate, this occurs at much higher maturity levels, typically $R_o = 2.0\%$, than does secondary gas generation in source rocks which starts at $R_o = 1.2\%$ (Horsfield et al., 1992a; Schenk et al., 1997; Dieckmann et al., 1998).

The rate of gas generation in sedimentary basins is predicted using kinetic parameters that are calculated from laboratory pyrolysis data (Tissot, 1969; Espitalié et al., 1988; Schaefer et al., 1990; Ungerer, 1990; Dieckmann et al., 1998). Most kinetic models assume a fixed number of parallel first-order pseudo-reactions (or Gaussian distribution) linking precursor and product, and no attention is given to actual reactions because of the complexities involved.

Although a simple precursor–product scheme is used in these parallel reaction models, the generation process can be better divided into three fundamental stages for the purpose of the present discussion (Engler, 1913; Tissot, 1969; Braun and Rothman, 1975; Ungerer, 1990). These are the depolymerisation of kerogen to form a highly polar bitumen plus gas (1), the cracking of the bitumen to yield oil and gas (2) and the cracking of oil to yield gas (3):

$$K \underset{k_1}{\rightarrow} C_1 + B + G_1 \quad (1)$$

$$B \underset{k_2}{\rightarrow} C_2 + O + G_2 \quad (2)$$

$$O \underset{k_3}{\rightarrow} C_3 + G_3, \quad (3)$$

where K, mass of kerogen; B, mass of bitumen; C_i, mass of carbonaceous residue; O, mass of oil; G_i, mass of gas; k_i, first-order rate constant for the stated reaction.

Natural petroleums are rich in hydrocarbons because the first reaction (1) is rate limiting at geological heating rates (Braun and Rothman, 1975). Because the second reaction is rate limiting at laboratory heating rates, all laboratory pyrolysates are rich in polar compounds irrespective of kerogen type (Horsfield, 1997). It is therefore astounding that petroleum generation in nature can be predicted by laboratory pyrolysis, as is often the case for marine petroleum systems (Quigley et al., 1987; Ungerer and Pelet, 1987; Braun and Burnham, 1992; Pepper and Corvi, 1995; Schenk and Horsfield, 1998), because the prediction is for bitumen generation, not hydrocarbon generation. Clearly, the kinetic parameters describing thermal degradation reactions (1) and (2) must be closely similar, at least in the case of marine organic matter (Larter and Horsfield, 1993), or predictions of natural generation using laboratory pyrolysis would not be successful. The question nevertheless arises as to whether the bitumen always simply represents a short-lived transient phase in the cracking reaction pathway linking kerogen and hydrocarbons, or whether recombination reactions may predominate under certain circumstances. Evidence for combination reactions are to be found in the literature. For example, alkylation is enhanced in the presence of kerogen (Weres et al., 1988; Williams et al., 1988; Düppenbecker and Horsfield, 1990; Voigtmann et al., 1994; Dieckmann et al., 1998). The gross chemical composition of the bitumen-intermediate in (1) and (2) could determine whether cleavage or reformation pathways are preferred. Whereas kerogen derived from aquatic organisms is predominantly aliphatic, and its degradation is one of successive cracking reactions, as alluded to above, terrigenous kerogen is aromatic/phenolic (Larter and Senftle, 1985; Horsfield, 1989), and its reaction pathway could involve more recombinations. In this regard, coal cracks to yield C_{6+} liquids on pyrolysis (Espitalié et al., 1988; Forbes et al., 1991), but some of the same moieties are retained or recombined into the macromolecular structure during natural coalification (Schenk and Horsfield, 1998). Because a given moiety may be released as a volatile product in the case of cracking or be retained in the macromolecular network in the case of recombination, we propose that the kinetics of gas generation will be affected if either reaction pathway is predominant.

Here, we consider the role of recondensation reactions during organic maturation, especially in sedimentary rocks containing mixtures of terrigenous and marine kerogen (immature Hydrogen Index typically 150–300 mg HC/g TOC). Sediments of this type, corresponding to Jones's organic facies BC and C (Jones, 1987), make up a high proportion of the 10^{16} tons of organic carbon on Earth (NERC, 1989; Killops and Killops, 1993), and therefore play an important role in the global carbon cycle. We focus on gas generation from the Heather Formation, the lower member of the Upper Jurassic Viking Group, offshore Norway, which contains mixed marine and terrigenous organic matter (Thomas et al., 1985; Erdmann, 1999), and contrast its gas generating characteristics with those of the main petroleum source rock in the area, the Draupne Formation, the upper member of the Viking Group. Either or both of these formations are thought to have generated the gas found in Viking Graben reservoirs (Goff, 1983; Skålnes et al., 1993; Horstad et al., 1994; Chung et al., 1995; Kubala et al., 2003). Our work is primarily experimental, utilising a number of pyrolysis techniques to

deconvolute primary from secondary gas-forming contributions and to distinguish the effects of cracking and recombination reactions on gas generating potential.

2. Choice of samples

Based on a large geochemical data set (Erdmann, 1999), two conventional core samples, one from the terrestrially influenced Heather Formation and the other of the marine Draupne Formation, were chosen for the investigation. The Heather Formation sample contains kerogen belonging to Type III (Fig. 1). Under the microscope the organic matter is composed of a mixture of vitrinite, fusinite, liptinitic fluorescent amorphous organic matter and algal bodies. The Draupne Formation sample contains Type II kerogen (Fig. 1). Microscopic investigations confirm the presence of liptinite and only minor amounts of terrigeneous organic matter. The aforementioned features are typical of the Heather Formation across much of the Norwegian continental shelf (Thomas et al., 1985).

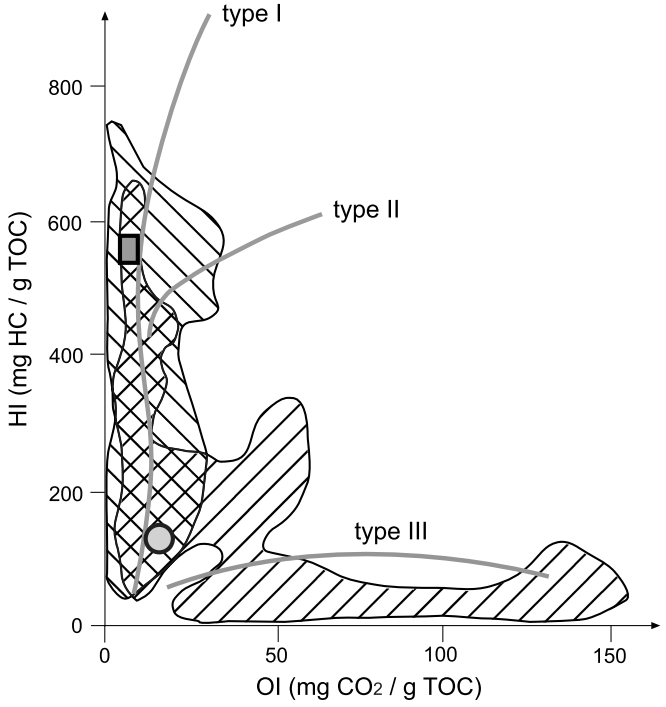

Fig. 1. Rock Eval parameters highlighting preference areas (Thomas et al., 1985) of Draupne (diagonal lines down to right) and Heather Formations (diagonal lines down to left) and composition of investigated Draupne (rectangle) and Heather Formation (circle) samples.

Dissolution of carbonates and silicates by HCl and HF treatment of the crushed rock samples resulted in the concentration of the organic matter by a factor of 3.7 to 5.6. The concentration procedure was followed by Soxhlet extraction at 60 °C for two days in order to remove the soluble organic matter. In doing so, errors in the subsequent kinetic analysis of the pyrolysis product yield curves, notably at the leading edge of generation curves, could be excluded. An azeotropic mixture of 23.4% methanol, 29.9% acetone and 47.6% chloroform was used. After air drying, the samples were heated for 2 min at 300 °C in flowing helium to remove all last traces of solvent. Geochemical screening data for the two samples are given in Table 1.

3. Experimental details

Four types of experiments were performed in order to define kinetic parameters for the generation of primary and secondary gas, and to analyse the reaction pathways involved.

3.1. "Rock Eval type" pyrolysis

This bulk flow pyrolysis method, showing no discrimination of gas versus oil potential, was used to gather data for calculating bulk petroleum kinetic parameters, as described by (Schaefer et al., 1990). Briefly, the two original samples were subjected to open system programmed-temperature pyrolysis at heating rates (0.1, 0.7 and 5.0 K min^{-1}) that were sufficiently low as to ensure correct temperature measurements (Schenk and Dieckmann, 2004) and sufficiently different for deriving a reasonable starting value of the frequency factor from the shift of peak generation temperatures. Temperatures were measured by a thermocouple located immediately above the sample. During pyrolysis a constant flow of argon (45 ml min^{-1}) was maintained in order to transport all pyrolysis products to the flame ionisation detector for the continuous registration of bulk pyrolysate (= petroleum) formation rates.

The bulk petroleum formation rate versus temperature curves were analysed assuming 26 first-order parallel reactions with activation energies regularly spaced between 45 and 70 kcal mol^{-1} and a single frequency factor. The parameters were optimized using a least-squares iteration method that compares measured and calculated formation rates at 300 temperatures until the corresponding error function presents a well-defined absolute minimum (Schenk et al., 1997).

Table 1
TOC, Vitrinite reflectance and Rock Eval screening data

fm	Sample	TOC (wt%)	R_o (%)	T_{max} (°C)	S1 (mg HC/g sample)	S2 (mg HC/g sample)	OI	HI	PI
Draupne	Core	11.9	0.37	428	2.77	59.76	4	502	0.04
Draupne	Extracted kerogen	44.8		423	3.15	248.50	7	555	0.01
Heather	Core	5.9	0.45	420	2.90	9.59	10	164	0.23
Heather	Extracted kerogen	33.1		421	1.50	48.28	7	146	0.03

The method was also applied to the residues of an artificially matured aliquot of the Heather Formation sample in order to compare bulk generation curves of mature and immature Heather Formation. Artificial maturation was brought about by heating the sample from 200 to 430 °C under MSSV conditions using a heating rate of 0.7 K min^{-1}.

3.2. Closed system configuration for simulating primary and secondary gas-forming reactions

Micro scale sealed vessel (MSSV) pyrolysis-gas chromatography (Horsfield et al., 1989) was used to gather the data from which the kinetic parameters of primary gas and secondary gas formation were calculated. More than 75 aliquots of each sample, each weighing 5–8 mg, were inserted into MSSV glass tubes (1.3 cm length, inner diameter approximately 1 mm, volume of 40 μl) and pyrolysed using a high precision standalone furnace. The temperature programme employed heating rates of 0.1, 0.7 and 5.0 K min^{-1} and started at 200 °C. Samples were removed from the oven every 5, 10 or 20 °C in the temperature interval of 300–620 °C. Subsequently, each aliquot was introduced into the Quantum Thermal Analysis System© which consisted of a heated piston device for breaking open the charged vessels, a cryogenic trap for focussing the released products, and a gas chromatograph equipped with a 25 m HP1 column (0.32 mm diameter and 0.5 μm film thickness) and flame ionisation detector (FID). Total product (integrated to column blank, Tables 2 and 3) and resolved product (skim baseline) amounts and more than 80 different compounds belonging to the normal alkane, branched alkane, aromatic hydrocarbon, alkylthiophene and alkylphenol classes were quantified (Erdmann, 1999) with reference to an external *n*-butane standard. In the current communication, the terms *gaseous* and *liquid* products refer to C_{1-5} and C_{6+} boiling ranges, respectively.

Hydrocarbon yields measured at the three different heating rates were approximated by spline functions, which were numerically differentiated in order to produce formation rate versus temperature curves (Horsfield et al., 1992a; Schenk et al., 1997; Dieckmann et al., 1998). These curves were then analysed as described above for calculation of the kinetic parameters.

3.3. Analytical open system configuration for simulating primary gas-forming reactions

During closed system pyrolysis, both primary and secondary gas generation take place. In order to gain a better understanding about primary gas evolution a multistep open system pyrolysis approach was adopted. The analyses were performed on 10 aliquots of each sample at a heating rate of 5.0 K min^{-1} (Table 4). The temperature program started at 300 °C and ended with temperatures between 350 and 570 °C. Pyrolysis was conducted on-line within

Table 2
Draupne Formation, MSSV pyrolysis product yields (μg/g sample) measured at three different heating rates

Heating rate:	0.1 K min^{-1}			0.7 K min^{-1}			5.0 K min^{-1}	
Temperature	C_{1-5}	C_{6+}	Temperature (°C)	C_{1-5}	C_{6+}	Temperature (°C)	C_{1-5}	C_{6+}
300	306	1470	302	219	800	300	126.9	2193
310	480	3022	330	503	2556	350	465	3380
320	743	6075	360	1616	12298	370	853	6214
333	1320	11086	375	3404	28555	390	1947	12471
340	1787	14326	390	5682	43324	400	3199	24309
350	2937	26210	400	9374	72337	410	4776	38435
360	4811	42150	410	13866	94306	420	6877	50339
370	7609	55923	420	20231	111420	425	8328	61671
380	13082	87042	425	24144	129155	430	9905	63638
390	20440	113505	430	29731	139284	435	12753	84234
395	23345	103490	440	39095	130741	440	14708	90415
401	29664	118279	445	45244	131472	445	16620	95685
405	36754	131837	450	55763	134300	450	20500	99327
410	44111	138153	455	62808	126989	455	23519	113113
415	46048	130893	460	71848	119405	460	27578	116185
420	53098	122528	465	78625	100713	470	37816	114090
425	63992	121916	470	85928	96546	475	42153	102777
430	73691	121414	480	112886	79893	480	48269	103919
440	72012	95798	490	137089	67060	490	60563	93498
445	108738	97306	495	129406	56459	500	67825	83839
450	127965	87985	520	122620	39759	510	82034	72639
460	136924	63046	540	111974	32235	530	104612	62745
470	150628	50372	560	101129	21576	550	111446	48635
480	135908	41326	580	101123	15154	570	109478	40262
490	125272	33068	600	101636	12248	610	93395	22021
510	114774	25584	620	103600	5326	630	98497	20050
540	103556	16934						

Table 3
Heather Formation, MSSV pyrolysis product yields (μg/g sample) measured at three different heating rates

Heating rate:	0.1 K min^{-1}			0.7 K min^{-1}			5.0 K min^{-1}	
Temperature (°C)	C_{1-5}	C_{6+}	Temperature (°C)	C_{1-5}	C_{6+}	Temperature (°C)	C_{1-5}	C_{6+}
300	350	668	300	400	829	350	508	1669
310	420	827	325	495	1067	370	730	2358
320	504	1046	350	691	1539	390	1010	2908
330	675	1573	370	1120	2639	400	1349	2995
340	833	1943	380	1505	3703	410	1811	4841
350	1195	2871	390	1966	4190	420	2026	5225
360	1589	3544	400	2552	4800	425	2444	5964
370	2271	4554	410	3156	5378	430	2790	6779
380	3062	5373	420	3741	5260	435	3040	5192
390	3791	4741	425	4022	4971	440	3372	6268
400	4826	4384	430	4563	4837	445	3643	6375
405	5221	4393	435	4895	4956	450	3879	6264
410	5765	4262	440	5683	5298	460	4486	6116
420	7337	4513	445	6023	4874	470	5396	6076
425	7757	4111	450	6497	4639	475	5721	6026
430	8733	4082	455	7110	5090	480	5911	5791
440	9213	3241	460	7367	3736	490	6971	5451
445	9920	3522	470	8893	4018	500	7852	4442
450	10485	3332	480	9771	3661	510	8739	4907
460	11573	3339	490	9975	3021	530	9741	4086
470	12124	2873	510	11628	2673	550	11130	3916
480	14140	2742	530	12745	2305	570	13022	3304
490	14334	2108	560	17459	2186	600	16521	3195
515	18157	2025				620	21144	2478
540	21969	1544						

Table 4
Multistep open system pyrolysis yields (μg/g sample) measured at 5.0 K min^{-1}

Draupne			Heather		
Temperature (°C)	C_{1-5}	C_{6+}	Temperature (°C)	C_{1-5}	C_{6+}
370	868	4545	350	406	715
400	2748	18195	370	508	603
410	3801	26957	390	1107	2119
420	6026	50730	410	1811	4248
430	9105	63725	430	3236	8938
440	12341	91502	450	5011	13946
450	15578	101708	470	6366	12633
470	20055	115757	490	8704	17947
490	26843	122061	510	9960	19872
530	30895	131212	540	11528	22725
			570	11990	20656

the piston device, rather than off-line. Tests using the Posidonia Shale and Draupne Formation (test data not reported in detail here) showed that for a heating rate of 5.0 K min^{-1}, the difference in the temperature fields was too small to produce any significant errors in the hydrocarbon formation curves, and therefore that the results of open and closed system could be compared directly with one another.

3.4. Preparative open system configuration for characterisation of C_{6+} pyrolysate

Some preparative experiments were performed to study the formation of bitumen (in Eq. (1)) in more detail. Open system pyrolysis products (300–600 °C at 60 K min^{-1}) were trapped in dichloromethane, and their composition determined by gas chromatography–mass spectrometry after solvent evaporation.

Aliquots of this isolated bitumen were sealed in MSSV vessels and pyrolysed to temperatures of 425 and 510 °C at 0.7 K min^{-1} after having removed all traces of solvent by thermovaporisation at 300 °C for 2 min under helium flow. The contents of the vessels were analysed using the gas chromatographic method described above.

4. Results and discussion

4.1. Deconvoluting primary versus secondary gas generation

4.1.1. Draupne Formation

We begin by presenting the results for the Draupne Formation since this unit is commonly thought to be a well-understood source rock in terms of oil and gas generation and may therefore serve as a model against which results obtained from the Heather Formation sample can be compared. The evolution profiles of total MSSV pyrolysis yields, and of the gas and liquid boiling range fractions (Table 2), shift to higher temperatures with increasing heating rates (Fig. 2A) in accordance with kinetic theory (Jüntgen and Van Heek, 1970). Total product yields reach cumulative plateaus, after which decreasing amounts at very high temperatures indicate the formation of coke during the cracking of wet gas (C_{2-5}) to methane. The C_{6+} boiling range reaches a maximum for each heating rate

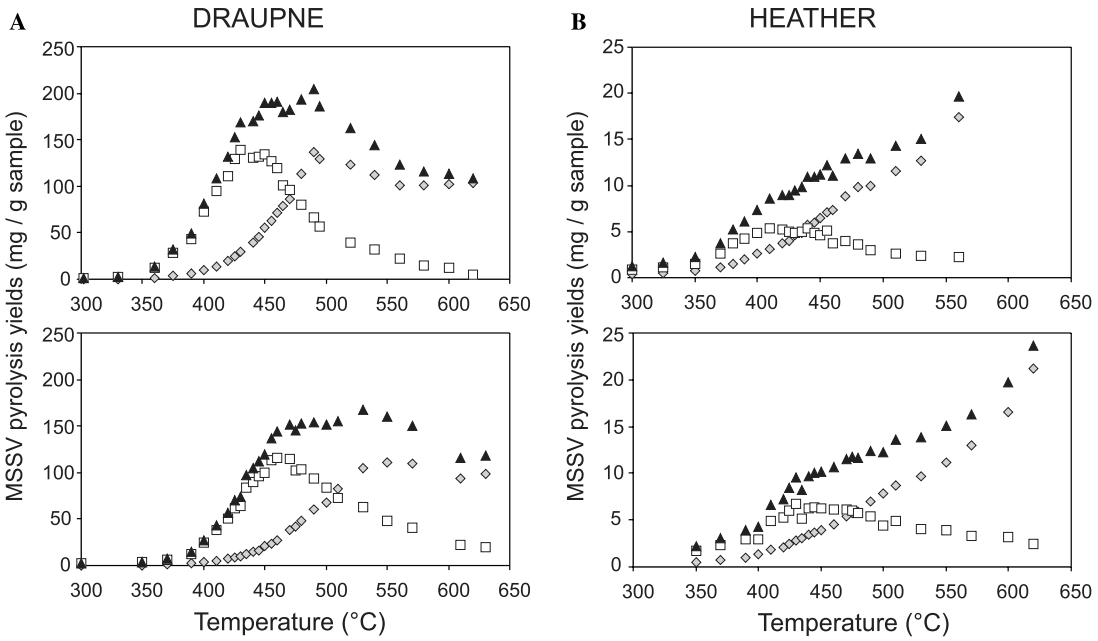

Fig. 2. MSSV pyrolysis cumulative yields for total products (full triangles), oil C_{6+} (open squares) and total gas C_{1-5} (rhombi) at heating rates of 0.7 K min^{-1} (top) and 5.0 K min^{-1} (bottom).

and subsequently decreases due to the formation of secondary gas and coke. Similar results have already been reported for other organic-rich Type II source rocks (Dieckmann et al., 1998, 2000).

Both generative and destructive processes occur during MSSV pyrolysis. With increasing thermal stress, high molecular weight aliphatic hydrocarbons undergo chain shortening and aromatic hydrocarbons increase in relative concentration, so that the final products at the highest thermal stress conditions are methane, benzene, naphthalene and a hydrogen poor macromolecular residue (Horsfield et al., 1992a). Secondary cracking is exemplified in its simplest form by the decrease of the boiling range fraction C_{6+} to form C_{1-5} in Fig. 2. Of course, a proportion of the measured total gas C_{1-5} must be primary products derived from the degradation of kerogen as well as those coming from secondary cracking. According to the approach of Dieckmann et al. (1998) this proportion can be estimated using simple stoichiometric assumptions demanded by the hydrogen balance Eq. (4). The degradation of a stoichiometric average oil is assumed to produce secondary gas (C_{1-5}) and coke in the simplest case (Sweeney et al., 1987; Braun and Burnham, 1992).

$$CH_{2.2} \rightarrow xCH_{3.2} + (1-x)CH_{0.2} \tag{4}$$

with $x \sim 0.7$, where $CH_{2.2}$ = assumed average composition of C_{6+}, $CH_{3.2}$ = assumed average composition of secondary gas C_{1-5}, $CH_{0.2}$ = assumed average composition of coke.

The assumed average compositions are hypothetical and can be adapted to different scenarios. Skjervøy and Sylta Ø (1993) for example used a conversion factor of $x = 0.5$ in their studies, whereas (Braun and Burnham (1992) used 0.605.

Based on these prerequisites, the formation of secondary gas can be calculated by Eq. (5). The amount of secondary gas (A_{sec}) for a given temperature (T_x) equals the difference of the amount of C_{6+} hydrocarbons at the cumulative maximum ($A_{C6+}(T_o)$) and the amount of C_{6+} hydrocarbons for an increased temperature ($A_{C6+}(T_x)$) times the conversion factor 0.7. The amount of primary gas (A_{pri}) can then be calculated using Eq. (6); it is simply the "remaining" gas when subtracting the calculated secondary gas from the total amount of gas (A_{tot}).

$$A_{sec}(T_x) = [A_{C6+}(T_0) - A_{C6+}(T_x)] \times 0.7 \tag{5}$$

$$A_{pri}(T_x) = A_{tot}(T_x) - A_{sec}(T_x). \tag{6}$$

It was initially assumed that the formation of gas by secondary cracking starts at the temperature of the cumulative maximum of the C_{6+} fraction (Sweeney et al., 1987; Schaefer et al., 1990; Horsfield et al., 1992a; Dieckmann et al., 1998). This approach has been successfully applied to the secondary gas generation of the kerogen Type II containing Toarcian Shale (Dieckmann et al., 1998) where the remaining gas was confirmed to be of primary origin by direct comparison to gas yield curves from multistep open system pyrolysis. In this context Berner et al. (1995) outlined that the primary cracking of the kerogen structure to form gas could be simulated by open system pyrolysis based on isotopic variations in hydrocarbon gases. For this reason, the open system pyrolysis-gas (C_{1-5}) is considered to be a reasonable measure for the amounts of primary gas.

However, when Draupne Formation C_{6+} generation profiles from MSSV (Table 2) were compared with multistep open system pyrolysis (Table 4) it was clear that oil to gas cracking starts before the primary generation of C_{6+} products had ended (Fig. 3). Both curves display the

gc-detectable fraction of oil-like C_{6+} pyrolysate produced from comparable but slightly different heating devices (see analytical section). The curves show excellent agreement up to temperatures of 460 °C. Starting from this point the closed system product curve decreases indicating that secondary cracking overcompensates primary generation, which is represented by the still increasing open system yield curve. The amount of secondary gas as estimated by the aforementioned approach should therefore be an underestimate; the amount of C_{6+} available for the cracking to secondary gas is the difference between the open and closed pyrolysis yields (Fig. 3).

As a consequence Eq. (5) was modified to Eq. (7) by replacing the amount of C_{6+} products at the cumulative maximum (A_{C6+} (T_0)) with the amount of observed primary C_{6+} products (A_{op} (T_x)) for any temperature T_x greater than T_0.

$$A_{sec}(T_x) = \left[A_{op}(T_x) - A_{C6+}(T_x)\right] \times 0.7. \quad (7)$$

The corresponding primary gas generation (total measured gas minus the calculated amount of secondary gas) (Eq. (6)) is now compared to the primary gas generation as detected by the multistep open system pyrolysis (Fig. 4). Results are in good agreement with regard to onset, increase and end of generation although the calculated primary gas curve shows somewhat higher yields then observed by open system pyrolysis. This indicates that secondary gas yields might still be slightly underestimated probably due to secondary gas generation starting before the C_{6+} maximum is reached in closed pyrolysis.

4.1.2. Heather Formation

The case of the Heather Formation is fundamentally different. Although the evolution profiles of the different product fractions still shift to higher temperatures with increasing heating rates (Fig. 2B), the total product and C_{1-5} gas yield curves continue to climb even at the highest experimental temperatures. Product compositions are clearly more gas dominated and the decay of the C_{6+} curve is very slow. As discussed below, the major phase of gas generation takes place at very high maturities and originates from the breakdown of a bitumen-intermediate formed during the earlier phases of maturation.

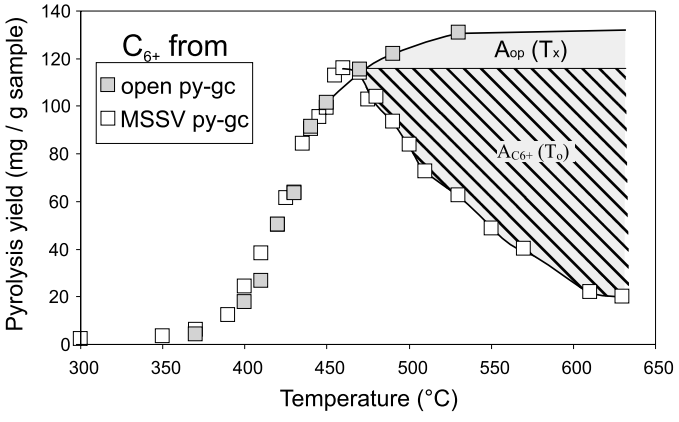

Fig. 3. Comparison of open and closed system C_{6+} product versus temperature curves at 5 K min^{-1} (Draupne Formation). The onset of secondary cracking indicated by the cumulative maximum (MSSV data at 460 °C) occurs before primary generation ends. Therefore, secondary gas yields will be underestimated if being based on the amounts of C_{6+} at the cumulative maximum A_{C6+} (T_0) (diagonal lines). Here, the amount of oil being cracked to gas was estimated using the difference of the open and closed pyrolysis yield curves (total grey area).

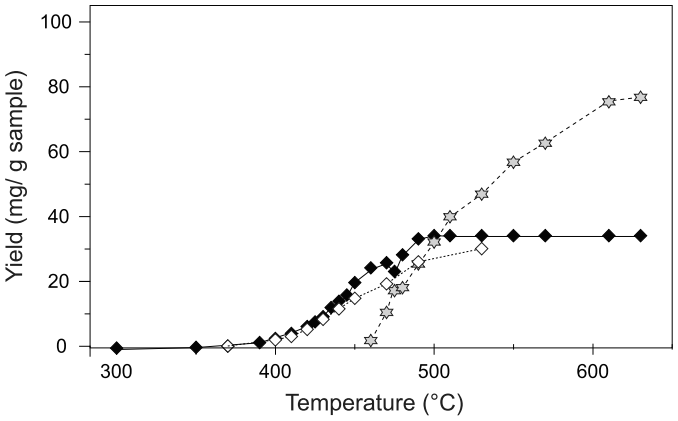

Fig. 4. Total MSSV pyrolysis gas yields minus the calculated amounts of secondary gas give the calculated primary gas curve (black diamonds) which is compared here to the gas yield curve detected by multistep open system pyrolysis (white diamonds) and shows generally good agreement. Lower observed primary gas yields between 450 and 530 °C can imply that secondary gas generation is still somewhat underestimated, shown for comparison as grey stars (all curves at 5.0 K min^{-1}).

The open and closed system C_{6+} formation curves (Fig. 5) reveal significant differences to observations made for the Draupne Formation sample (Figs. 3 and 4). The difference between yields generated under open and closed pyrolysis conditions is much greater. Also the temperature difference between the closed system C_{6+} maximum and the end of C_{6+} generation from open system pyrolysis is quite large, and approximately 125 °C. The estimated amount of secondary gas resulting from the degradation of oil is very small based on the stoichiometric calculation, and consequently the "remaining" gas makes up the major proportion of products. It is clear from an excellent agreement with observed open system yields up to 550 °C that the remaining gas is of primary origin, but only up to that temperature. At higher temperatures there is a steep increase in gas yield which cannot be attributed to a primary source but also cannot be attributed to the cracking of volatile C_{6+} components either.

4.2. Recombination reactions

Both features, namely the significant gap between open and closed system C_{6+} curves and the mismatch between the observed and calculated gas generation profiles at high temperatures, can be explained by a proportion of C_{6+} compounds, visible in the open system, recombining with

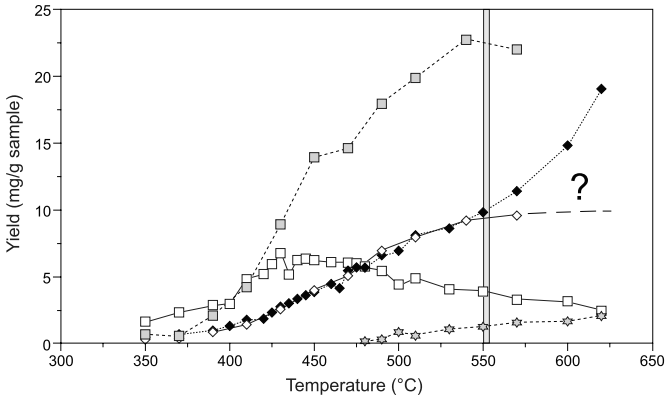

Fig. 5. Heather Formation MSSV pyrolysis measured C_{6+} (open squares) and calculated secondary (grey stars) and primary gas (black diamonds) versus multistep open system pyrolysis C_{6+} oil (grey squares) and C_{1-5} gas (white diamonds) at 5.0 K min^{-1}. Note the strong deviation of calculated versus observed primary gas at temperature higher than 550 °C (indicated by ?). The vertical bar indicates the end of primary generation observed by open system Rock Eval type bulk flow pyrolysis.

the kerogen in the closed system to form a high molecular residue. This material is thermally very stable and only degrades to give gas at very high temperatures. The phenomenon can be explained in terms of chain reaction terminations according to the Rice-Kossiakoff mechanism (Kossiakoff and Rice, 1943). Simple retention or polymerisation (Solomon and Rosser, 1965) of C_{6+} products on mineral surfaces with subsequent cracking are considered to be unlikely processes because the clay and pyrite assemblages which remain after kerogen concentration have not brought about comparable effects in other studies, including those of the Posidonia Shale, Duvernay Formation (Dieckmann et al., 1998, 2000) and Draupne Formation (this publication). It would appear that the observed process is a specific feature of terrigenous organic matter. A further argument for the recombination of C_{6+} moieties with the kerogen structure might be the observation of Bakr et al. (1991), that the amount of free radicals, initially generated by cracking reactions, decreases (their stage 2) after the initially increasing trend. The authors assign this behaviour to radical recombination reactions with no related weight loss, a feature which fits well with the observations reported here.

In order to test the recombination hypothesis, the approach of Schenk and Horsfield (1998) was applied. Briefly, these authors compared the natural and artificial maturation of two different kerogen types. In the case of a natural maturation series of the marine Posidonia Shale kerogen, products were thought to have been released by thermal cleavage because product formation rate curves obtained by Rock Eval type pyrolysis of mature samples fell completely within the formation curve envelope of the least mature sample. This was explained by pseudo-component potentials having been stripped away in the order of increasing activation energy as maturation proceeded. In stark contrast the mature formation curves for a Westphalian coal sample series fell outside of the immature envelope due to the formation of new, more stable activation energy potentials ostensibly by aromatisation and condensation reactions. The residue had an enhanced thermal stability which would not be predicted by evaluation of the immature sample.

With these considerations in mind, Rock Eval type open system pyrolysis was performed on an artificially matured (MSSV pyrolysis to 430 °C at 0.7 K min^{-1}) Heather Formation aliquot and formation rate curves were compared with those of the immature sample (Fig. 6). The measured formation rate curve of the mature sample is outside the immature envelope (Fig. 6A and B), with an even more significant shift observed when extrapolated to a geological heating rate of 10^{-11} K min^{-1} (Fig. 6C and D). The increased stability can be explained in terms of newly formed material exhibiting higher activation energy potentials, as observed for the maturation of Westphalian coal reported by Schenk and Horsfield (1998). It must be noted however that the amount of newly formed matter indicated by the area lying outside the immature formation rate curve is smaller than expected from the results of MSSV pyrolysis. The reason for this difference is most likely that the recombination process is not completed at the simulated degree of maturation.

To fully test the significance of the recombination process for naturally matured samples, it would be necessary to find a sample set of homogenous Heather Formation covering a broad natural maturity range (cf. Schenk and Horsfield, 1998). Unfortunately, this was not possible because of the heterogeneous character of the organic matter in the Heather Formation (Thomas et al., 1985; Skjervøy and Sylta Ø, 1993), compounded by sampling and age dating problems (Kubala et al., 2003). For instance, the petrological observation of a non-detritial solid bitumen in a deep sample from the Møre Basin at maturities as high as 1.3% R_o (Erdmann, 1999) could represent either

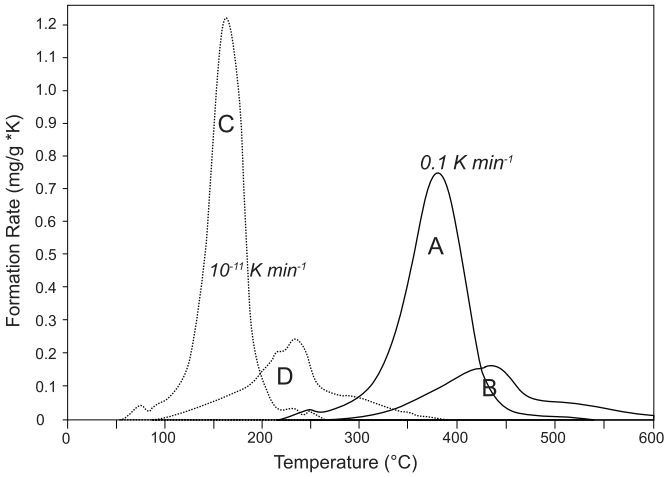

Fig. 6. Formation rate versus temperature curves for an immature (A) sample and an artificially matured (B) aliquot of Heather Formation at a laboratory heating rate of 0.1 K min^{-1} and extrapolated to geologic heating conditions of 10^{-11} K min^{-1} (C and D).

recombination residues of first formed C_{6+} compounds or simply represent the residue of an unexpelled oil.

Therefore, the experimental approach was extended to examine some of the molecular changes accompanying artificial maturation. In particular the fate of open system pyrolysis products under confined conditions and with increasing temperature was considered. First, an open system preparative pyrolysis experiment (300–600 °C; 50 K min^{-1}) was performed in order to collect C_{6+} products in a solvent trap. The concentrated material (C_{12+}) was then heated under MSSV conditions to the temperature at which the maximum C_{6+} yield was observed earlier (425 °C at 0.7 K min^{-1}), but in the absence of residual kerogen. Product compositions were then compared with those from kerogen pyrolysis under the same heating conditions, where pyrolysate-residual kerogen interactions could have taken place (Fig. 7). A second set of experiments was conducted at a higher temperature (510 °C). This step was thought to simulate secondary cracking to form gas. Striking differences were noted for both heating stages. Whereas for the kerogen (Fig. 7, left side) the main products are simple mono- and diaromatic hydrocarbons and mono- and dimethylated phenols, the pyrolysis of the bitumen (Fig. 7, right side) formed predominantly saturated hydrocarbons with a maximum in chain length at about *n*-C18 to *n*-C20 and a great variety of polyalkylated aromatic and phenolic components. Thus, contributions of long alkyl-moieties, alkyl-aromatics and -phenols seem to be involved in pyrobitumen formation as these components do not appear in the pyrolysate of kerogen. In other words,

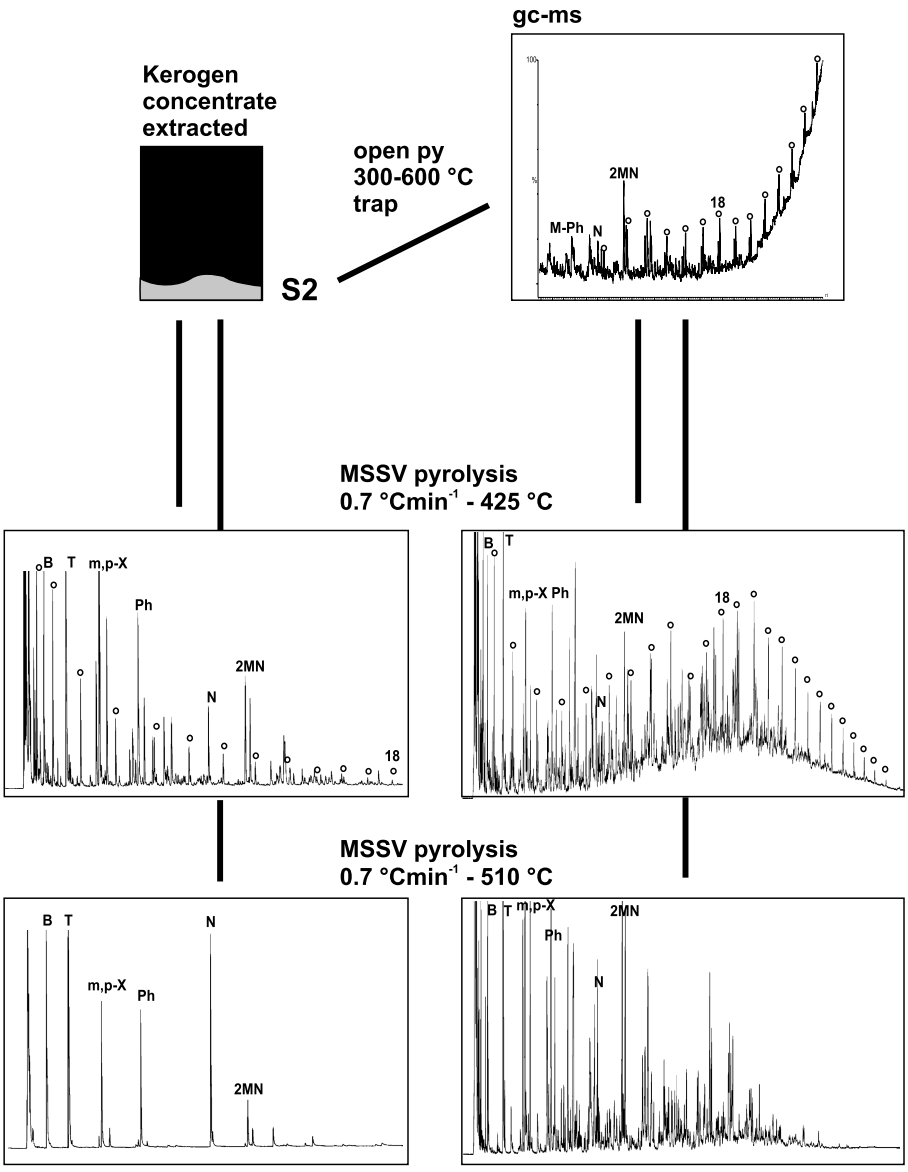

Fig. 7. Preparative experiment to investigate how bitumen reacts to heating in the presence (left) and absence (right) of kerogen. Products are stripped from the kerogen by open system pyrolysis and trapped. In a next step they undergo MSSV pyrolysis to temperatures of 425 and 510 °C at 0.7 K min^{-1}. Products are compared to MSSV pyrolysate obtained from the kerogen concentrate at the same temperatures. Annotation of peaks: open circles, alkyl moieties; B, benzene; T, toluene; m,p-X, meta, para Xylene; Ph, phenol; N, naphthalene, 2MN, 2-methylnaphthalene.

n-alkyl moieties are present in the original kerogen and released on pyrolysis in the liquid fraction, but secondary reactions between the bitumen and the residual kerogen lead to the neoformation of an insoluble solid bitumen. It is this bitumen or recombination residue which we think is the source of the late stage secondary gases.

It is noteworthy that the original oil potential, as signified by the abundance of *n*-alkyl chains in pyrolysis products (Larter and Senftle, 1985; Horsfield, 1989), is lost because of recombination reactions involving the first-formed bitumen and the kerogen residue in the case of the Heather Formation. Phenolic and aromatic ring systems in the parent kerogen appear to play a key role in incorporating *n*-alkyl chains into recombination structures, ostensibly via cyclisation and aromatisation reactions. Extensive aromatisation of Type II kerogen has already been reported for the Alum Shale and the Bakken Shale, and is in these cases related to the presence of unusual precursor biota and/or the effects of alpha-ray bombardment (Lewan and Buchardt, 1989; Horsfield et al., 1992b; Muscio et al., 1994). By stark contrast, *n*-alkyl moieties in predominantly paraffinic-naphthenic-aromatic systems (Horsfield, 1989), such as in Draupne Formation organic matter, remain as free unbound substances, and are released as part of liquid petroleum in nature.

4.3. Timing of gas generation in geological systems

Using the calculated primary and secondary gas generation curves (Figs. 4 and 5) as well as the high temperature gas from the cracking of recombination residues at three heating rates, sets of kinetic parameters were determined, comprising individual frequency factors and activation energy distributions. The determination was done according to published routines (Schaefer et al., 1990). The generation of gas from these processes is summarised in a model (Fig. 8K and L) showing laboratory measurements and a prediction to geological heating conditions based on individual kinetic parameters for each type of gas.

For the Heather Formation (K), primary gas generation (A) covers a broader temperature window than does oil generation, with peak generation at the end of the oil window at approximately 190 °C. Secondary gas generation (B) from primary preserved liquids is of minor importance and takes place after oil generation ceases, maximising at 220 °C. Late stage gas generation from the purported recombination residue source (C) is extremely prolific, though the small number of data points for the recombination residue cracking made an accurate determination of kinetic parameters impossible. Nevertheless, the preservation of the relative order of oil, primary and secondary gas implies an extrapolation to very high geological temperatures of approximately 250 °C for peak generation. Except for secondary gas generation from recombination residues, predictions based on open and closed system devices are in good agreement. This is in contrast to the Draupne Formation (L), where 10–15 °C higher

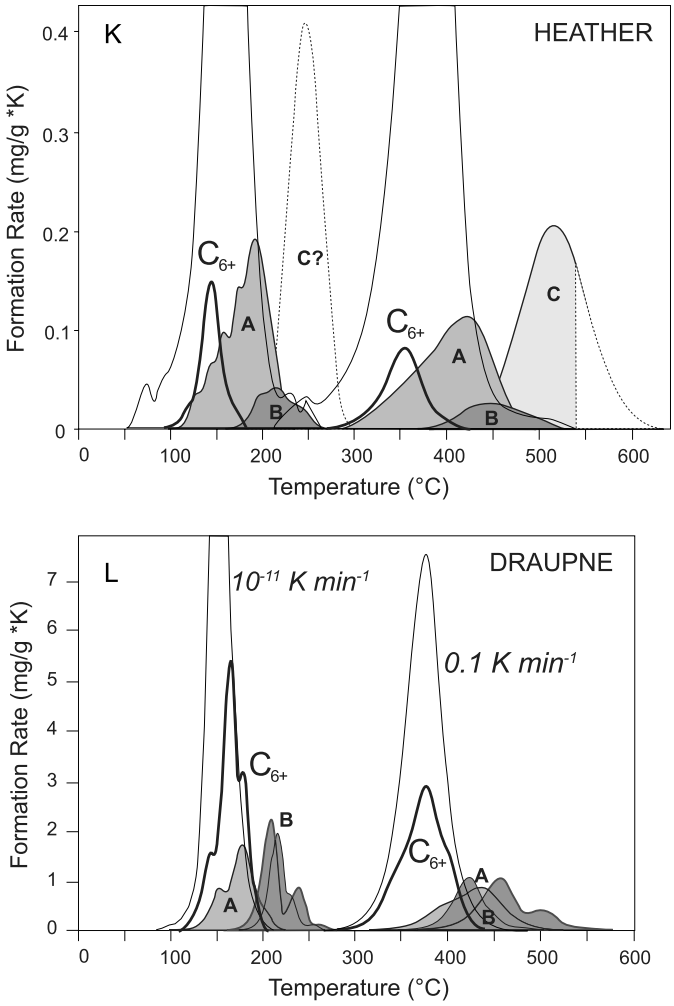

Fig. 8. Compilation of results showing laboratory curves and extrapolated results. Rock Eval pyrolysis bulk kinetic curves are depicted as thin lines without fill. MSSV pyrolysis curves include oil (C_{6+}) and primary (A) and secondary (B) gas as well as the high temperature secondary gas for the case of the Heather Formation (C).

temperatures result for predictions based on MSSV data than for data from the open system pyrolysis. There are also differences observed between the laboratory and the geological order of product formation. For example, at laboratory heating rate the relative generation order of oil, primary and secondary gas is observed for the Draupne Formation, as for the Heather Formation. However, when extrapolated to geological rates, the primary gas generation of the Draupne Formation is shifted to lower temperatures, so that oil and primary gas generation occurs together in a similar temperature window of 120–200 °C. Secondary gas generation from first-formed liquid products takes place mostly after oil generation ceased.

4.4. Implications for the Norwegian shelf

We have deduced that recombination reactions take place during the artificial maturation of a Type III kerogen, and that the thermally stable macromolecular residue

formed in this way is the source of appreciable amounts of dry gas at very high temperatures (Table 5). The obvious inference is that an increased potential for late gas generation exists in the deep reaches of many Norwegian sedimentary basins and possibly in other deep sedimentary basins around the world as well. In Fig. 9, potential areas in the northern North Sea are highlighted where the deepest Upper Jurassic sediments can occur and where very late gas generation from neocondensed macromolecules could play a role for basin-fill type source rocks containing mixed marine–terrigeneous kerogen. The kinetic uncertainties are too great to accurately predict the upper temperature limit to which this late stage of gas generation extends, but the fact that generation occurs at and above 250 °C adds a new dimension to prospectivity along the Norwegian continental shelf.

Another important implication for deep basins is the timing of petroleum charge. Often oil and gas generation are rather early with respect to trap formation, meaning that petroleum pools will not occur because the oil or gas evolves before a feasible pool for trapping the resource is available. Here, the possibility of a late gas charge can increase prospectivity especially in cases of late formed petroleum traps at shallow stratigraphic levels. The maturity history graph for the Upper Jurassic (Fig. 10) in a pseudowell location offshore Norway (Fig. 9) shows that vitrinite reflectance (R_o) of more than 2.0% will be reached in the Upper Jurassic units during Tertiary times in the deep parts of the basin. This is the maturity interval in which cracking of recombination residues is postulated. The gas generation window is compared to time intervals which result from commonly accepted maturity intervals for oil and gas generation (Tissot and Welte, 1978; Hunt, 1979) which would

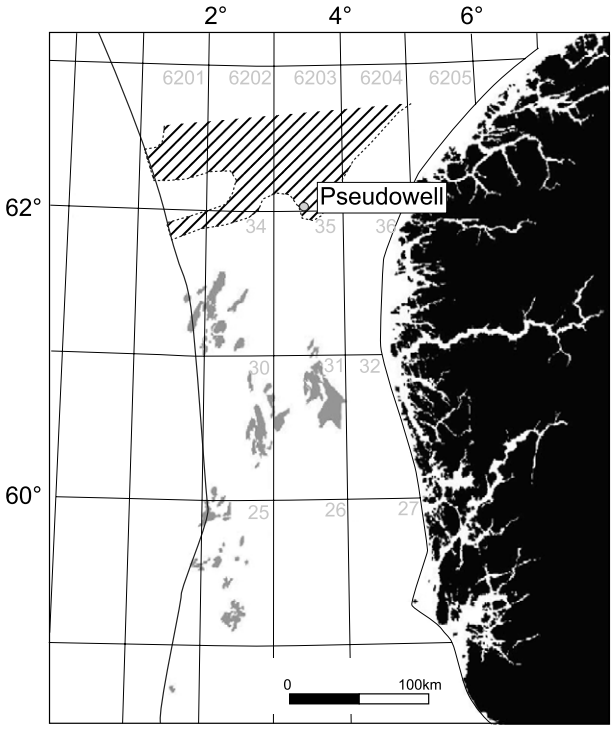

Fig. 9. Norwegian North Sea. Areas where late gas generation from recombination residue cracking might occur in lean Upper Jurassic sediments. Pseudowell location for 1D maturation history graph in Fig. 10.

Table 5
Heather Formation, MSSV pyrolysis gas product yields (μg/g sample) measured at three different heating rates

Heating rate:	0.1 K min^{-1}			0.7 K min^{-1}			5.0 K min^{-1}	
Temperature (°C)	C_1	C_{2-5}	Temperature (°C)	C_1	C_{2-5}	Temperature (°C)	C_1	C_{2-5}
300	41	235	300	25	296	350	49	359
310	58	271	325	49	352	370	95	468
320	82	313	350	100	475	390	190	654
330	146	413	370	252	712	400	267	878
340	170	520	380	356	956	410	395	1177
350	311	758	390	481	1258	420	379	1281
360	429	1014	400	703	1653	425	539	1559
370	653	1440	410	944	2012	430	719	1796
380	908	1958	420	1199	2390	435	821	1938
390	1227	2407	425	1356	2521	440	953	2125
400	1720	2960	430	1596	2817	445	1072	2294
405	1943	3149	435	1818	2947	450	1213	1519
410	2290	3377	440	2192	3329	460	1547	2695
420	3197	4036	445	2466	3453	470	2071	3159
425	3613	4029	450	2755	3517	475	2223	3268
430	4291	4329	455	3125	3737	480	2444	3241
440	5038	4087	460	3536	3721	490	3195	3571
445	5752	4078	470	4712	4032	500	3933	3708
450	6425	3998	480	5674	3953	510	4667	3867
460	7879	3617	490	6466	3396	530	6348	3276
470	9208	2875	510	9184	2353	550	8483	2629
480	11610	2479	530	11334	1330	570	10999	1968
490	12766	1538	560	16745	603	600	15352	1123
515	17630	463				620	20502	623
540	21774	290						

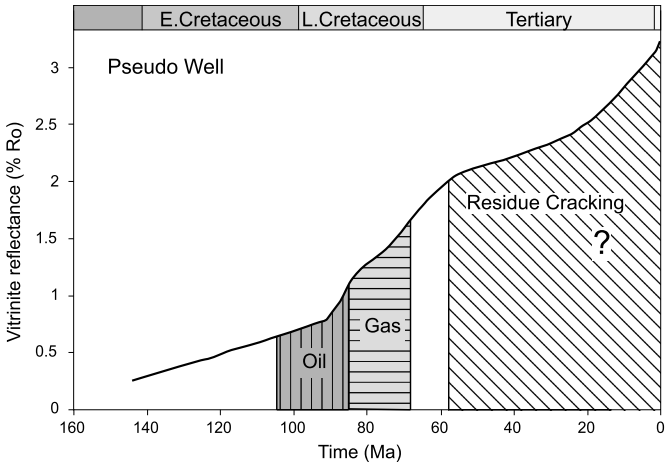

Fig. 10. Maturation history for a potential deep Heather Formation source rock in the pseudowell location (Fig. 9). Conventional oil and gas generation windows are marked to highlight the late generation timing for recombination residue cracking. Uncertainty of the exact timing due to lack of precise kinetic parameters are indicated by question mark. The graph was calculated using standard 1D basin modelling.

be predicted to occur mainly during Late Cretaceous times. Such early generated petroleum could be lost from the sedimentary basin by seepage if trapping pools evolved at times later than Cretaceous, whereas trapping of the late gas charge could still be possible.

5. Conclusions

Two types of kerogen have been analysed in this study: the Draupne Formation whose kerogen (Type II) is largely aliphatic and to some degree thiophenic, and the Heather Formation whose kerogen (Type III) is more aromatic and in part phenolic (Erdmann, 1999). Fitting the classical model of sequential thermal cracking reactions, the Draupne Formation generates two types of gas, primary gas generated directly from macromolecular precursors, and secondary gas generated from the cracking of primary liquids. Kinetic models already exist for quantifying their respective generation in time and space (e.g. Dieckmann et al., 1998). The Heather Formation generates an additional type of gas which evolves at very high geological temperatures. The source of the gas is not part of the original kerogen, and is therefore not directly inherited from biological precursors. It is a thermally stable bitumen which forms at relatively low levels of maturation via recombination reactions involving the liquid products co-generated with primary gas. The cracking of highly stable substituents from the recombined bitumen, ostensibly via the alpha cleavage of methyl groups, is the main gas-forming pathway for this type of organic matter.

We predict that temperatures in excess of 200 °C, corresponding to depths greater than ca. 6 km in the offshore Norway area, are required to generate the gas in sedimentary basins via this mechanism. From an exploration perspective, basin-fill sediments may constitute a potentially prolific source of free gas in deep basins. The same scenario is expected to apply to fluviodeltaic source rocks where terrestrial organic matter predominates.

Only closed system pyrolysis can evaluate the reported high temperature gas potential because the recombination reactions which form the gas generating precursors can be simulated. By contrast, the same liquid products taking part in the reaction under closed system conditions are simply swept away and detected under open system conditions, thereby overestimating liquid (“oil”) potential and severely underestimating gas potential.

Acknowledgments

Norsk Hydro and Saga Petroleum especially Nigel Mills, Nils Telnæs and Arnd Wilhelms are acknowledged for providing the sample set and their support and permission to publish the data. The work was carried out, as part of Michael Erdmann’s Ph.D studies at Forschungszentrum Jülich. The scientific advice from Hans-Joachim Schenk, now retired, and the technical support of Franz Leistner are gratefully acknowledged. Tanja Barth, Robert C. Burrus and 2 anonymous reviewers are thanked for their comments which improved the manuscript.

Associate editor: Robert C. Burruss

References

Bakr, M., Akiyama, M., Sanada, Y., 1991. In situ high temperature ESR measurements for kerogen maturation. *Org. Geochem.* **17**, 321–328.

Berner, U., Faber, E., Scheeder, G., Panten, D., 1995. Primary cracking of algal and landplant kerogens: kinetic models of isotope variations in methane, ethane and propane. *Chem. Geol.* **126**, 233–245.

Braun, R.L., Rothman, A.J., 1975. Oil shale pyrolysis. Kinetics and mechanisms of oil production. *Fuel* **54**, 129–131.

Braun, R.L., Burnham, A.K., 1992. PMOD: a flexible model of oil and gas generation, cracking and expulsion. *Org. Geochem.* **19**, 161–172.

Chung, H.M., Claypool, G.E., Walters, C.C. 1995. Multiple origins of petroleum in the Viking Graben. In: 17th Int. Meeting on Org. Geochem., San Sebastian, pp. 505–511.

Cooles, G.P., Mackenzie, A.S., Quigley, T.M., 1986. Calculation of petroleum masses generated and expelled from source rocks. *Org. Geochem.* **10**, 235–245.

Cornford, C., 1994. Mandal-Ekofisk(!) petroleum system in the Central Graben of the North Sea. In: Magoon, L.B., Dow, W.G. (Eds.), *The Petroleum System from Source to Trap*. American Association of Petroleum Geologists, pp. 537–571.

Dieckmann, V., Schenk, H.J., Horsfield, B., 2000. Assessing the overlap of primary and secondary reactions by closed- versus open-system pyrolysis of marine kerogens. *J. Anal. Appl. Pyrol.* **56**, 33–46.

Dieckmann, V., Schenk, H.J., Horsfield, B., Welte, D.H., 1998. Kinetics of petroleum generation and cracking by programmed-temperature closed-system pyrolysis of Toarcian Shale. *Fuel* **77**, 23–31.

Düppenbecker, S., Horsfield, B., 1990. Compositional information for kinetic modelling and petroleum type prediction. *Org. Geochem.* **16**, 259–266.

England, W.A., Mackenzie, A.S., 1989. Some aspects of the organic geochemistry of petroleum fluids. *Geologische Rundschau* **78**, 291–303.

Engler, K.O.V. 1913. *Die Chemie und Physik des Erdöls*, vol. 1. Leipzig, S.Hirzel.

Erdmann, M. 1999. Gas generation from overmature Upper Jurassic source rocks, northern Viking Graben. Berichte des Forschungszentrums Jülich; 3700. Dissertation RWTH Aachen.

Espitalié, J., Ungerer, P., Irwin, I., Marquis, F., 1988. Primary cracking of kerogens. Experimenting and modeling C1, C2-C5, C6-C15 and C15+ classes of hydrocarbons formed. *Org. Geochem.* **13**, 893–899.

Forbes, P.I., Ungerer, P.M., Kuhfuss, A.B., Riis, F., Eggen, S., 1991. Compositional modeling of petroleum generation and expulsion: trial application to a local mass balance in the Smørbukk Sør field, Haltenbanken Area, Norway. *Am. Assoc. Petr. Geol. Bull.* **75**, 873–893.

Goff, J.C., 1983. Hydrocarbon generation and migration from Jurassic source rocks in the East Shetland Basin and Viking Graben of the Northern North Sea. *J. Geol. Soc. Lond.* **140**, 445–472.

Horsfield, B., 1989. Practical criteria for classifying kerogens: some observations from pyrolysis-gas chromatography. *Geochim. Cosmochim. Acta* **53**, 891–901.

Horsfield, B., 1997. The bulk composition of first-formed petroleum in source rocks. In: Welte, D.H. et al. (Eds.), *Petroleum and Basin Evolution*. Springer-Verlag, Berlin Heidelberg, pp. 337–402.

Horsfield, B., Disko, U., Leistner, F., 1989. The micro-scale simulation of maturation: outline of a new technique and its potential applications. *Geologische Rundschau* **78**, 361–374.

Horsfield, B., Schenk, H.J., Mills, N., Welte, D.H., 1992a. An investigation of the in-reservoir conversion of oil to gas: compositional and kinetic findings from closed-system programmed-temperature pyrolysis. *Org. Geochem.* **19**, 191–204.

Horsfield, B., Bharati, S., Larter, S.R., Leistner, F., Littke, R., Mann, U., Schenk, H.J., Dypvik, H., 1992b. On the atypical petroleum generating characteristics of alginite in the Cambrian Alum Shale. In: Schidlowski, M.E.A. et al. (Eds.), *Early Organic Evolution: Implications for Mineral and Energy Resources*. Springer-Verlag, Berlin Heidelberg, pp. 257–266.

Horstad, I., Larter, S.R., Mills, N. 1994. Migration of hydrocarbons in the Tampen Spur area, Norwegian North Sea—a reservoir geochemical evaluation. In: Cubitt, J.W., England, W.A. (Eds.), *The Geochemistry of Reservoirs*. Geological Society Special Publication 86, pp.159–184.

Hunt, J.M., 1979. *Petroleum Geochemistry and Geology*. Freeman and Company, San Francisco, p. 617.

Jones, R.W., 1980. Some mass balance and geological constraints on migration mechanisms. In: Roberts, W.H., Cordell, R.J. (Eds.), *Problems of Petroleum Migration*, vol. 10. AAPG Studies in Geology, American Association of Petroleum Geologists.

Jones, R.W., 1987. Organic facies. In: Brooks, J., Welte, D.H. (Eds.), *Advances in Petroleum Geochemistry 2*. Academic Press, London, pp. 1–90.

Jüntgen, H., Van Heek, K.H., 1970. Reaktionsabläufe unter nichtisothermen Bedingungen. In: Davison, A., Dewar, M.J.S., Hafner, K., Heilbronner, E., Hofmann, U., Niedenzu, K., Schaefer, K., Wittig, G. (Eds.), *Fortschritte der chemischen Forschung*, vol. 13. Topics in Current Chemistry, pp. 603–699.

Killops, S.D., Killops, V.J., 1993. *An Introduction to Organic Geochemistry*. Longman Scientific and Technical, Harlow.

Kossiakoff, A., Rice, F.O., 1943. Thermal decomposition of hydrocarbons, resonance stabilisation and isomerization of free radicals. *J. Am. Chem. Soc.* **65**, 590–595.

Krooss, B.M., Leythaeuser, D., Lillack, H., 1993. Nitrogen rich natural gas. *Erdöl, Kohle – Erdgas-Petrochem* **46**, 271–276.

Kubala, M., Bastow, M., Thompson, S., Scotchman, I., Øygard, K., 2003. Geothermal regime, petroleum generation and migration. In: Evans, D. et al. (Eds.), *The Millenium Atlas: Petroleum Geology of the Central and Northern North Sea*. The Geological Society of London, pp. 289–315.

Larter, S.R., Senftle, J.T., 1985. Improved kerogen typing for petroleum source rock analysis. *Nature* **318**, 277–280.

Larter, S.R., Horsfield, B., 1993. Determination of structural components of kerogens by the use of analytical pyrolysis methods. In: Engel, M.H., Macko, A. (Eds.), *Organic Geochemistry*. Plenum Press, New York, pp. 271–287.

Lewan, M., Buchardt, B., 1989. Irradiation of organic matter by uranium decay in the Alum Shale, Sweden. *Geochim. Cosmochim. Acta* **53**, 1307–1322.

Mackenzie, A.S., Quigley, T.M., 1988. Principles of geochemical prospect appraisal. *Am. Assoc. Petr. Geol. Bull.* **72**, 399–415.

Mann, U., Hantschel, T., Schaefer, R.G., Krooss, B., Leythaeuser, D., Littke, R., Sachsenhofer, R.F., 1997. Petroleum migration: mechanisms, pathways, efficiencies and numerical simulations. In: Welte, D.H. et al. (Eds.), *Petroleum and Basin Evolution*. Springer-Verlag, Berlin Heidelberg, pp. 405–520.

Monin, J.C., Connan, J., Oudin, J.L., Durand, B., 1990. Quantitative and qualitative experimental approach of oil and gas generation: application to the North Sea source rocks. *Org. Geochem.* **16**, 133–142.

Muscio, G.P.A., Horsfield, B., Welte, D.H., 1994. Occurrence of thermogenic gas in the immature zone—implications from the Bakken in-source reservoir system. *Org. Geochem.* **22**, 461–476.

NERC (National Environment Research Council)/ Marine Sciences Directorate, 1989. Oceans and the global carbon cycle, an introduction to the biogeochemical ocean flux study of NERC Marine Sciences Directorate, Plymouth Marine Laboratory.

Pepper, A.S., Corvi, P.J., 1995. Simple kinetic models of petroleum formation. Part III: modelling an open system. *Mar. Petrol. Geol.* **12**, 417–452.

Quigley, T.M., Mackenzie, A.S., Gray, J.R., 1987. Kinetic theory of petroleum generation. In: Doligez, B. (Ed.), *Migration of hydrocarbons in sedimentary basins*. Editions Technip, pp. 649–666.

Santamaria-Orozco, D., Horsfield, B., 2004. Gas generation potential of Upper Jurassic (Tithonian) source rocks in the Sonda de Campeche, Mexico. In: Bartolini, C., Buffler, R.T., Blickwede, R.F. (Eds.), *The Circum-Gulf of Mexico and the Caribbean: Hydrocarbon habitats, Basin Formation and Plate Tectonics*, vol. 79. AAPG Memoir, pp. 349–363.

Schaefer, R.G., Schenk, H.J., Hardelauf, H., Harms, R., 1990. Determination of gross kinetic parameters for petroleum formation from Jurassic source rocks of different maturity levels by means of laboratory experiments. *Org. Geochem.* **13**, 115–120.

Schenk, H.J., Horsfield, B., 1998. Using natural maturation series to evaluate the utility of parallel reaction kinetics models: an investigation of Toarcian shales and Carboniferous coals, Germany. *Org. Geochem.* **29**, 137–154.

Schenk, H.J., Dieckmann, V., 2004. Prediction of petroleum formation: the influence of laboratory heating rates on kinetic parameters and geological extrapolations. *Mar. Petrol. Geol.* **21**, 79–95.

Schenk, H.J., di Primio, R., Horsfield, B., 1997. The conversion of oil into gas in petroleum reservoirs. Part 1: comparative kinetic investigation of gas generation from crude oils of lacustrine, marine and fluviodeltaic origin by programmed-temperature closed-system pyrolysis. *Org. Geochem.* **26**, 467–481.

Skålnes E., Patience R.L., Bjørlykke K., Karlsen D.A., 1993. Petroleum geochemistry and filling history of the Hild field, Norwegian Continental Shelf. In: Øygard, K. (Ed.), *Organic Geochemistry*. Poster sessions from the 16th International Meeting on Organic Geochemistry, Stavanger, p. 51.55.

Skjervøy, A., Sylta, Ø., 1993. Modelling of expulsion and secondary migration along the southwestern margin of the Horda Platform. In: Doré, A.G., et al. (Eds.) *Basin Modelling: Advances and Applications*, NPF Special Publication 3, pp. 499–537.

Solomon, D.H., Rosser, M.J., 1965. Reactions catalysed by minerals. Part 1: polymerisation of styrene. *J. Appl. Polym. Sci.* **9**, 1261–1271.

Sweeney, J.J., Burnham, A.K., Braun, R.L., 1987. A model of hydrocarbon generation from Type I kerogen: application to Uinta basin, Utah. *Am. Assoc. Petr. Geol. Bull.* **71**, 967–985.

Thomas, B.M., Møller-Pedersen, P., Whitaker, M.F., Shaw, N.D., 1985. Organic facies and hydrocarbon distributions in the Norwegian North Sea. In: Thomas, B.M. et al. (Eds.), *Petroleum Geochemistry in Exploration of the Norwegian Shelf*. Norwegian Petroleum Society, Graham & Trotman, pp. 3–26.

Tissot, B., 1969. Premières données sur les mécanismes et la cinétique de la formation du pétrole dans les sédiments.

Simulation d'un schema réactionnel sur ordinateur. *Rev. Inst. Fr. Pét* **24**, 470–501.

Tissot, B.P., Welte, D.H., 1978. *Petroleum Formation and Occurrence*. Springer Verlag, Berlin.

Ungerer, P., 1990. State of the art of research in kinetic modelling of oil formation and expulsion. *Org. Geochem.* **16**, 1–25.

Ungerer, P., Pelet, R., 1987. Extrapolation of the kinetics of oil and gas formation from laboratory experiments to sedimentary basins. *Nature* **327**, 52–54.

Voigtmann, M.F., Yang, K., Batts, B.D., Smith, J.W., 1994. Evidence for synthetic generation of methylphenanthrenes in sediments. *Fuel* **73**, 1899–1903.

Weres, O., Newton, A.OS., Tsao, L., 1988. Hydrous pyrolysis of alkanes, alkenes, alcohols and ethers. *Org. Geochem.* **12**, 433–444.

Wiese, K., Kvenvolden, K.A., 1993. Introduction to microbial and thermal methane. In: Howell, D.G. (Ed.), *The Future of Energy Gases*. US Geological Survey Professional Paper 1570, United States Government Printing Office, Washington, pp.13–21.

Williams, J.A., Dolcater, D.L., Torkelson, B.E., Winters, J.C., 1988. Anomalous concentrations of specific alkylaromatic and alkylcycloparaffin components in West Texas and Michigan crude oils. *Org. Geochem.* **13**, 47–59.